Вестник РУДН. Серия: Инженерные исследования
RUDN Journal of Engineering Research

2024;25(3):308–318

ISSN 2312-8143 (Print); ISSN 2312-8151 (Online)
journals.rudn.ru/engineering-researches

DOI: 10.22363/2312-8143-2024-25-3-308-318
UDC 528.8:528.7
EDN: ZMCNKM

Research article / Научная статья

Dynamics of Land Use, Land Cover Changes and Their Impacts on Land Surface Temperature Using Satellite Imagery

Temesghen E. Sereke[a,b]✉, Tumuzghi Tesfay[c,d], Vitaly V. Bratkov[a], Elsayed S. Mohamed[c,e], Dinh T. Quyen[a]

[a] Moscow State University of Geodesy and Cartography, *Moscow, Russia*
[b] College of Business and Social Sciences, *Adi Keih, Eritrea*;
[c] RUDN University, *Moscow, Russia*
[d] Hamelmalo Agricultural College, *Keren, Eritrea*
[e] National Authority for Remote Sensing and Space Sciences, *Cairo, Egypt*
✉ temesghensereke@gmail.com

Article history

Received: March 12, 2024
Revised: June 21, 2024
Accepted: July 3, 2024

Conflicts of interest

The authors declare that there is no conflict of interest.

Abstract. Population growth and urbanization have resulted in land use/land cover (LULC) changes and affect land surface temperature (LST), which contributes to global warming. The study aimed to detect the LULC changes across Mendefera, Eritrea, from 2002 to 2022, and examine their impacts on LST. Two Landsat-7 ETM and One Landsat OLI_TRI-8 images from 2002, 2012 and 2022 were utilized. A supervised vector machine algorithm was used to classify LULC. Overall accuracy and Kappa coefficient were calculated. Linear regression was performed to show the relationship between Normalized Difference Vegetation Index (NDVI) and LST. The study found remarkable LULC changes in the study area 2002–2022. Built-up and agricultural areas increased by 113.5 and 64.4% respectively, whereas natural vegetation and open areas decreased by 77.6 and 24.8%, respectively. The highest and lowest mean LST were recorded in built-up (35°C) and natural vegetation (29.7°C) areas, respectively. Generally, mean LST decreased by 3.3°C in the study area from 2002 to 2022, and a negative correlation was observed between NDVI and LST. Thus, the study concludes that urbanization causes vegetation degradation, abrupt built-up growth and urban heat islands. The study will help planners and decisions-makers in planning appropriate mechanisms in land use planning and climate change mitigation.

Keywords: land use/land cover, land surface temperature, overall accuracy, Kappa coefficient

Authors' contribution

Seredke T.E. — development of a research plan, methodology, map creation; *Tesfay T.* — introductory part, revision of the results, development of graphics; *Quyen D.T.* — formula verification, accuracy assessment for land use maps; *Bratkov V.V., Mohamed E.S.* — editing of the manuscript, revision of the manuscript according to the comments of experts.

For citation

Sereke TE, Tesfay T, Bratkov VV, Mohamed ES, Quyen DT. Dynamics of land use, land cover changes and their impacts on land surface temperature using satellite imagery. *RUDN Journal of Engineering Research.* 2024;25(3):308–318. http://doi.org/10.22363/2312-8143-2024-25-3-308-318

Мониторинг влияния на температуру поверхности суши динамики землепользования, изменения растительного покрова

Т.Э. Сереке[a,b]✉, Т. Тесфай[c,d], В.В. Братков[a], Э.С. Мохамед[c,e], Д.Т. Куин[a]

[a] Московский государственный университет геодезии и картографии, *Москва, Россия*
[b] Колледж бизнеса и социальных наук, *Ади Кейх, Эритрея*
[c] Российский университет дружбы народов, *Москва, Россия*
[d] Сельскохозяйственный колледж Дамельмало, *Керен, Эритрея*
[e] Национальное управление по дистанционному зондированию и космическим наукам, *Каир, Египет*
✉ temesghensereke@gmail.com

История статьи

Поступила в редакцию: 12 марта 2024 г.
Доработана: 21 июня 2024 г.
Принята к публикации: 3 июля 2024 г.

Заявление о конфликте интересов

Авторы заявляют об отсутствии конфликта интересов.

Аннотация. Рост населения и урбанизация привели к изменениям в растительном покрове, которые влияют на температуру поверхности суши, что способствует глобальному потеплению. Цель исследования — выявление изменений в растительном покрове в Мендефере, Эритрея, за период с 2002 по 2022 г. и изучение их влияние на температуру поверхности суши. Были использованы два снимка Landsat-7 ETM и один снимок Landsat OLI_TRI-8, сделанные в 2002, 2012 и 2022 гг. Для классификации изменений в растительном покрове применен алгоритм управляемой векторной обработки. Рассчитаны коэффициенты достоверности и коэффициент Каппа. Для отображения взаимосвязи между нормализованным вегетационным индексом и температурой поверхности суши сгенерирована линейная регрессия. В ходе исследования отмечены значительные изменения растительного покрова в исследуемой области в 2002–2022 гг. Площадь застройки и сельскохозяйственных угодий увеличилась на 113,5 и 64,4 % соответственно, в то время как естественная растительность и открытые пространства сократились на 77,6 и 24,8 % соответственно. Самый высокий и самый низкий средние значения изменений в растительном покрове отмечены в населенных пунктах (35 °C) и естественной растительности (29,7 °C) соответственно, но в целом средние значения изменений в растительном покрове снизились на 3,3 °C в исследуемой области с 2002 по 2022 г., и наблюдалась отрицательная корреляция между нормализованным вегетационным индексом и изменениями в растительном покрове. Таким образом, сделан вывод о том, что урбанизация приводит к деградации растительности, резкому росту застройки и появлению городских островов тепла. Исследование поможет специалистам по планированию и лицам, принимающим решения, разработать соответствующие механизмы для планирования землепользования и смягчения последствий изменения климата.

Ключевые слова: землепользование, температура поверхности Земли, общая точность, коэффициент Каппа

Вклад авторов

Сереке Т.Э. — разработка плана исследования, методологии, создание карт; *Тесфай Т.* — вводная часть, доработка результатов, разработка графики; *Куин Д.Т.* — проверка формул, оценка точности для карт землепользования; *Братков В.В., Мохамед Э.С.* — редактура рукописи, доработка рукописи по замечаниям экспертов.

Для цитирования

Sereke T.E., Tesfay T., Bratkov V.V., Mohamed E.S., Quyen D.T. Dynamics of land use, land cover changes and their impacts on land surface temperature using satellite imagery // Вестник Российского университета дружбы народов. Серия: Инженерные исследования. 2024. Т. 25. № 3. С. 308–318. http://doi.org/10.22363/2312-8143-2024-25-3-308-318

Introduction

Since the second half of the 20th century, the world population has shown rapid increase from 2.6 billion to 7.7 billion and likely to reach around 9.9 billion by the year 2050 [1]. Different studies revealed that about 66% of the global population is expected to be stacked in urban areas in 2050 [2; 3]. Population growth and urbanization are among the prominent factors that affect land surface. The major driving forces for the changes that happened to land use land cover changes (LULCC) are mainly due to anthropogenic activities [4], which may also affect LST and global warming. Therefore, LULC change detection could help understanding LST changes [5; 6] and take proper actions to mitigate global warming. The application of Remote Sensing and GIS in LULC changes detection is effective, appropriate, ultimate, and timely. Different techniques and algorithms have already been developed for LULC classification, including support vector machine (SVM), maximum likelihood (ML), random forest/random tree, deep learning, etc. SVM is one of the powerful classification algorithms for identifying the boundaries of features by dividing and screening the classes [7], solving different problems in relation to regression and groups [8], and arriving at conclusions with limited training samples [9; 10]. Suggests that [8] reported that SVM classifier in both ArcGIS Pro and Google Earth Engine exhibited the best performance compared to the maximum likelihood, random forest/random tree, classification and regression trees, and minimum distance classifiers.

In urban areas, LULC change due to rapid urbanization is the main reason for the increased LST [4]. Suggests that [2] analyzed the dynamics in LULC change and its impact on LST for Galle City, Sri Lanka, and reported that built-up area increased by 38%, whereas vegetation and non-built-up area reduced by 26% and 12%, respectively, and LST increased by 3.2˚C from 1996 to 2019. Suggests that [11] studied the spatiotemporal relations between LULC change and LST for Tehran, Iran, and they found that impervious surface area increased by 48.27%, vegetated land decreased by 7.10%, and mean LST has increased by 2–3˚C at the city center and 5–7˚C at the periphery between 1988 and 2018. Also reported [12] notable rise in mean LST of 4.5˚C (summer) and 5.7˚C (winter) in Sialkot city, Pakistan, due to urbanization from 1989 to 2020. On the contrary, [13] reported that LST decreased by 0.56˚C from 2000 to 2020 across the Kanyakumari district, India. Linear regression was performed to show the correlation between LST and NDVI [6]. Normalized Difference Vegetation Index (NDVI) is one of the frequently used vegetation indices, which is calculated from multispectral bands using red, and near infrared and provides useful information for environmental monitoring, ecosystem conservation, urban green infrastructure, and others [14]. Correlation graphs between LST and NDVI have indicated negative relationship among them [6].

Eritrea is one of the six fastest urbanizing country in Africa and the ten fastest in the world.[1] More than 65% of Eritreans live in rural areas, while its annual urban population growth was 6% for the years 2000–2005 [15], and the numbers are expected to increase. In many areas of developing countries, rapid population increase has often resulted in LULC change [9; 15]; approximately 90% of population growth has been observed in

[1] United Nations. UN Department of Economic and Social Affairs Divisions. World Urbanization Prospects. The 2018 Revision: New York, USA, 2018.

Asia and Africa [16]. Studies on LULC dynamics and their impacts on LST are crucial in developing countries such as Eritrea for informed-policy decisions for land use planning and climate-change mitigation; however, there are no such studies in Eritrea. Thus, this study was carried out in Greater Mendefera to detect the dynamics of LULC changes and their associated impacts on LST between 2002 and 2022.

1. Materials and Methods

1.1. Study Area

Greater Mendefera, with geographic coordinates of $14^{0}53'8''$N and $38^{0}48'59''$E (its center), is located 54 km south of Asmara in Zoba Debub, Eritrea, within the moist highlands agroecological zone of Eritrea with 17.35°C mean monthly air temperature, 549 mm average annual rainfall and 1462.44 mm yr^{-1} potential evapotranspiration rate. Greater Mendefera includes the Mendefera city and surrounding villages. The government of Eritrea has provided a master plan for the Greater Mendefera 20 years ago, and the city expanded through different infrastructure projects. Mendefera city is the capital for both Zoba Debub and Sub-Zoba Mendefera. The settlers of the city are engaged in different economic activities, trade, services, farming, and so on. Mendefera, having favorable climatic conditions and fertile black soils in its surroundings, is known for its agricultural and dairy activities that produce different cereals, peas, beans, vegetables, and dairy products. Small-scale irrigated agriculture is common at the periphery and within the city. Many nearby farming villages surround the city. The surrounding area is highly populated because of its fertile black soils (Figure 1).

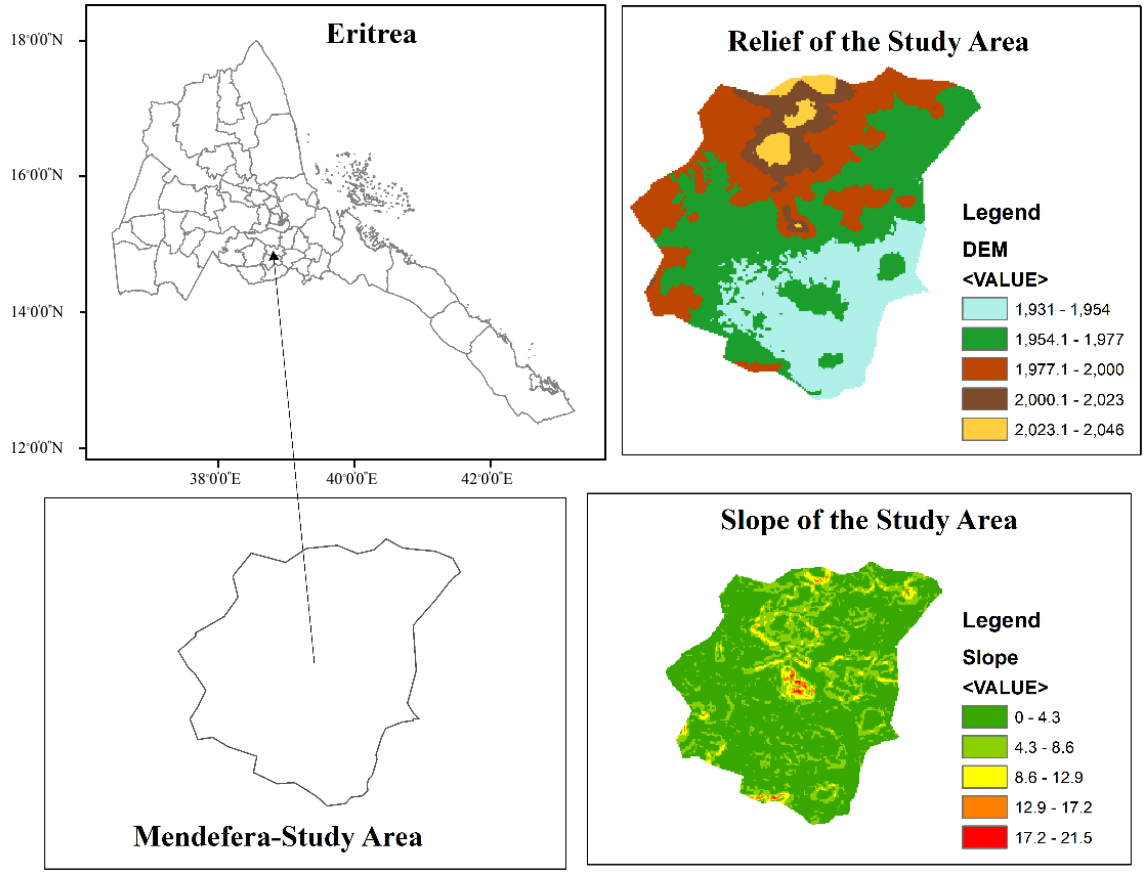

Figure 1. Location, DEM and slope of the study area
S o u r c e: made by T.E. Sereke

1.2. Data and Methodologies

To examine LULC changes, three Landsat images Combination-2 Level-2 of Landsat 8 OLI_TRI for 2022 and Landsat 7 ETM+ for the year 2002 and 2012 with WRS Path 169, Row 050 were downloaded from United States Geological Survey Earth Explorer. Composite Bands from Landsat images were analyzed to classify LULC. Thermal bands that are Band 6 for 2002 and 2012 and Band 10 for 2022 were extracted and analyzed to calculate LST of the study area. NDVI was calculated using Band 5 and Band 4 for Landsat 8, whereas Bands 4 and 3 were used for Landsat 7. Vector layer for the study area was extracted from the country's shape file that was obtained from EMIC-Eritrean Mapping and Information Center. In addition, ASTER-DEM was used to calculate the slope and Digital Elevation Model. All the spatial data were geo-referenced using UTM zone 37 N based on global WGS 84. All the images were preprocessed, processed and analyzed using ENVI 5.3, ArcGIS 10.8.2 and QGIS 3.28. The overall methodologies and procedures used in this study are shown in the flowchart in Figure 2.

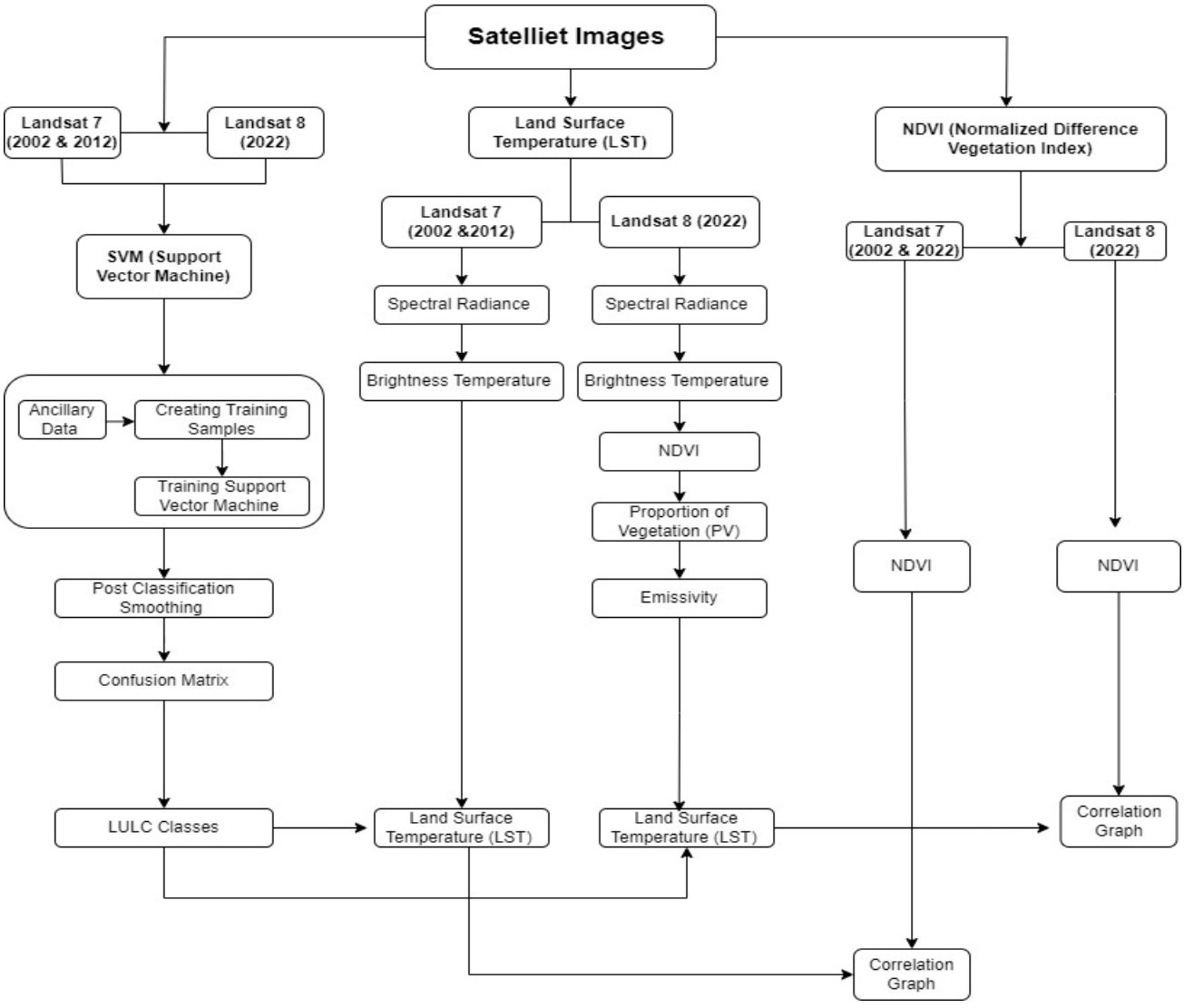

Figure 2. Flowchart showing the methodologies
S o u r c e: made by T.E. Sereke

1.3. Land Use / Land Cover Classification and Accuracy Assessment

LULC classification scheme proposed by AfriCover was adopted [17], and four dominant LULC classes were chosen in the study area: built-up, agricultural, natural vegetation, and open areas. The major LULC classes and their simplified explanations for the study area are listed in Table. In order to achieve high precision of LULC classification for the study area, composite bands with ancillary data were utilized. SVM algorithm was employed for LULC classification as it has many advantages [7–10], and the overall accuracy and kappa coefficient were culculated to assess the LULC classification accuracy.

Major LULC classes in the study area and their simplified explanations

No.	LULC Classes	Simplified Explanation
1.	Built-up Areas	Industrial, commercial and public built-ups; transportation and others
2.	Agricultural Areas	Any kind of rain-fed agriculture and irrigation
3.	Natural Vegetation	Seasonal wetlands, artificial trees and natural bushes and trees
4.	Open Area	An area left for fallow, grazing and other purposes

1.4. Land Surface Temperature Computation

Images for 2002, 2012, and 2022 were captured on 29 September 2002; 24 September 2012; and 28 September 2022 respectively. All images were captured in September to reduce variability.

LST for the year 2002 and 2012-Landsat 7. For Landsat 7, LST was estimated using Thermal Band 6. The following steps were used to convert Band 6 of Landsat 7 from DN to LST:

1. Conversion of DN to Radiance [18]

$$L_\lambda = \left(\frac{\mathrm{LMAX}_\lambda - \mathrm{LMIN}_\lambda}{\mathrm{QCALMAX} - \mathrm{QCALMIN}}\right) \times \times (\mathrm{QCAL} - \mathrm{QCALMIN}) + \mathrm{LMIN}_\lambda, \quad (1)$$

where L_λ is Spectral radiance, QCAL is Quantized Calibrated Pixel value in DN, LMAX_λ is Spectral radiance scaled to QCALMAX in (Watts/(m^2×sr×μm)), LMIN_λ is the spectral radiance scaled to QCALMIN in (Watts/(m^2×sr×μm)), QCALMIN is the minimum quantized calibrated pixel value (corresponding to LMIN_λ) in DN and QCALMAX is the maximum quantized calibrated value (corresponding to LMAX_λ) in DN.

2. Conversion of Radiance to *BT* [19]

$$BT = \frac{K_2}{\ln\left(\frac{K_1}{L_\lambda} + 1\right)} - 273.15, \quad (2)$$

where *BT* is Brightness temperature, which is effective at satellite temperature in Celsius, K_2 is Calibration constant 2, K_1 is Calibration constant 1, and L_λ is the spectral radiance in (Watts/(m^2×sr×μm) from (Equation 1).

1.5. Land surface temperature for 2022–Landsat 8

For Landsat 8, LST was estimated using thermal Band 10. The following steps were used to convert Band 10 of Landsat 8 from DN to Land Surface Temperature (LST):

TOA (Top of Atmospheric) spectral radiance was calculated using Equation 3 [19]

$$\mathrm{TOA}(L) = M_L \cdot Q_{cal} + \mathrm{A}_L, \quad (3)$$

where M_L refers to Band-specific multiplicative rescaling factor from the metadata (RADIANCE_MULT_BAND_*x*, where *x* is the band number), Q_{cal} refers to quantized calibrated value and A_L refers to Band-specific additive rescaling factor from the metadata (RADIANCE_ADD_BAND_*x*, where *x* is the band number).

The radiance values were converted into brightness temperature. It was calculated using Equation 4 [6]

$$T_B = \left(K_2 / \ln\left(K_1 / L\right) + 1\right) - 273.15, \quad (4)$$

where T_B is brightness temperature in Kelvin; K_1 refers to Band-specific thermal conversion constant from the metadata ($K1$_CONSTANT_BAND_***x***, where x is the thermal band number), K_2 refers to Band-specific thermal conversion constant from the metadata (K_2_CONSTANT_BAND_***x***, where x is the thermal band number) and L refers to TOA from (Equation 1).

The normalized difference vegetation index (NDVI) was calculated using Equation 5 [2; 5]

$$\mathrm{NDVI} = \frac{(\mathrm{NIR\text{-}RED})}{(\mathrm{NIR+RED})}, \quad (5)$$

where NIR and RED in Landsat 8 refer to the surface reflectance values of Band 5 and Band 4 respectively.

Proportion of vegetation was calculated using Equation 6 [2; 4]

$$P_v = \left(\frac{\mathrm{NDVI\text{-}NDVI_{min}}}{\mathrm{NDVI_{max}} - \mathrm{NDVI_{min}}} \right)^2, \quad (6)$$

where P_v is the proportion of vegetation, NDVI refers to normalized difference vegetation index, $\mathrm{NDVI_{min}}$ refers to the minimum values of NDVI and $\mathrm{NDVI_{max}}$ refers to the maximum values of NDVI.

Land surface emissivity was calculated using Equation 7 [2]:

$$\varepsilon = \{mP_v + n\}, \quad (7)$$

where ε is the land surface emissivity; m and n are the functions of soil emissivity and vegetation emissivity, respectively, for $m = 0.004$ and $n = 0.986^2$ [3]; and P_v is the amount of vegetation (Equation 4).

Land surface temperature was calculated using Equation 8 [2; 4]

$$\mathrm{LST} = T_B/1 + (\lambda \cdot T_B/p) \ln\varepsilon, \quad (8)$$

where T_B — brightness temperature in Celsius; λ — is the central-band wavelength of emitted radiance (10.895 μm for Band 10 [2]; p is $h \times c/\sigma$ ($1.438 \times 10{-}2$ m K), where σ is the Boltzmann constant ($1.38 \times 10{-}23$ J/K), h is Planck's constant ($6.626 \times 10{-}34$ Js), and c is the speed of light (3.0×108 m/s^{-1}) [4]; ε is land-surface emissivity estimated from (Equation 6) [2].

2. Results and Discussion

2.1. LULC Change Dynamics

The total study area was 2536 ha. In 2002, the areal coverages for open, agricultural, natural vegetation and built-up areas were 47.4, 28.3, 17.8, and 6.5%, respectively, whereas in 2022, they were 35.7, 46.5, 4.0, and 13.9%, respectively (Figure 3). The study noted remarkable LULC changes between 2002 and 2022. Built-up and agricultural areas increased by 186.8 ha (113.5%) and 461.8 ha (64.4%) and while natural vegetation and open areas decreased by 349.9 ha (77.6%) and 298.6 ha (24.8%), respectively (Figure 4). Natural vegetation was cleared for agricultural and construction activities, and open areas were converted to agriculture and infrastructures owing to population growth and urbanization. These findings are supported by reports that built-up area increased rapidly but vegetation area decreased [2; 11].

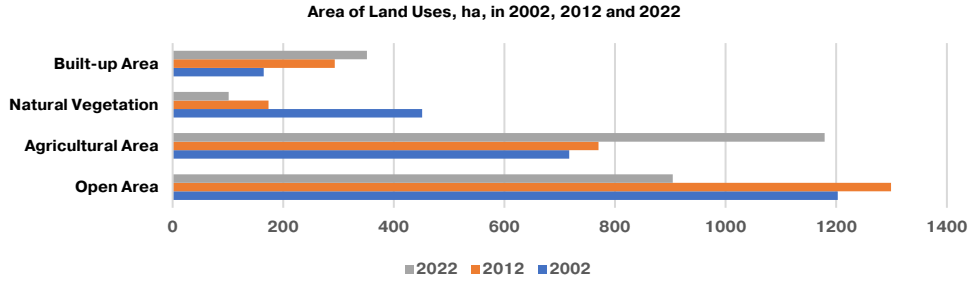

Figure 3. Land uses and their area, ha, in 2002, 2012 and 2022
S o u r c e : made by T. Tesfay

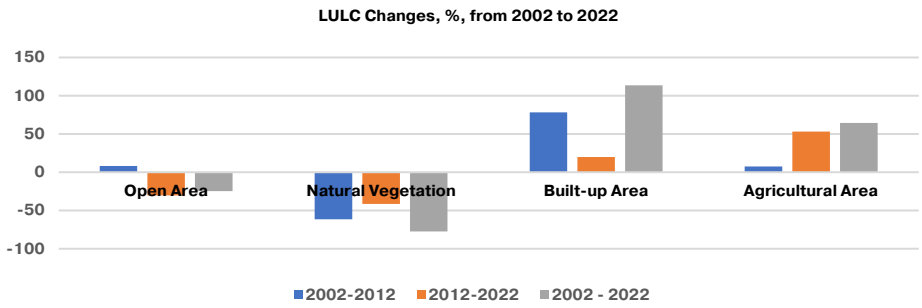

Figure 4. LULC changes, in 2002–2012, 2012–2022 and 2002–2022, %
S o u r c e: made by T. Tesfay

From 2002 to 2012, built-up, open, and agricultural areas increased by 128.5 ha (78.1%), 96.4 ha (8%) and 52.9 ha (7.4%), respectively, but natural vegetation area decreased by 277.8 ha (61.6%) (Figure 4). The high increase in build-up and high decrease in vegetation areas indicates that vegetation was cleared for construction purposes. Since the loss in the natural vegetation was greater, it is clear that vegetation was also cleared for agricultural and energy purposes, as an energy crisis is common in the study area. From 2012 to 2022, natural vegetation and open areas decreased by 72.1 ha (41.6%) and 395.0 ha (30.4%) while agricultural and built-up areas increased by 408.9 ha (53.1%) and 58.3 ha (19.9%), respectively (Figure 4).

The LULC classification was performed with good accuracy and precision. The overall accuracy and Kappa Coefficients for 2002, 2012 and 2022 were 89, 91 and 89%, and 0.84, 0.85 and 0.85, respectively (Figure 5).

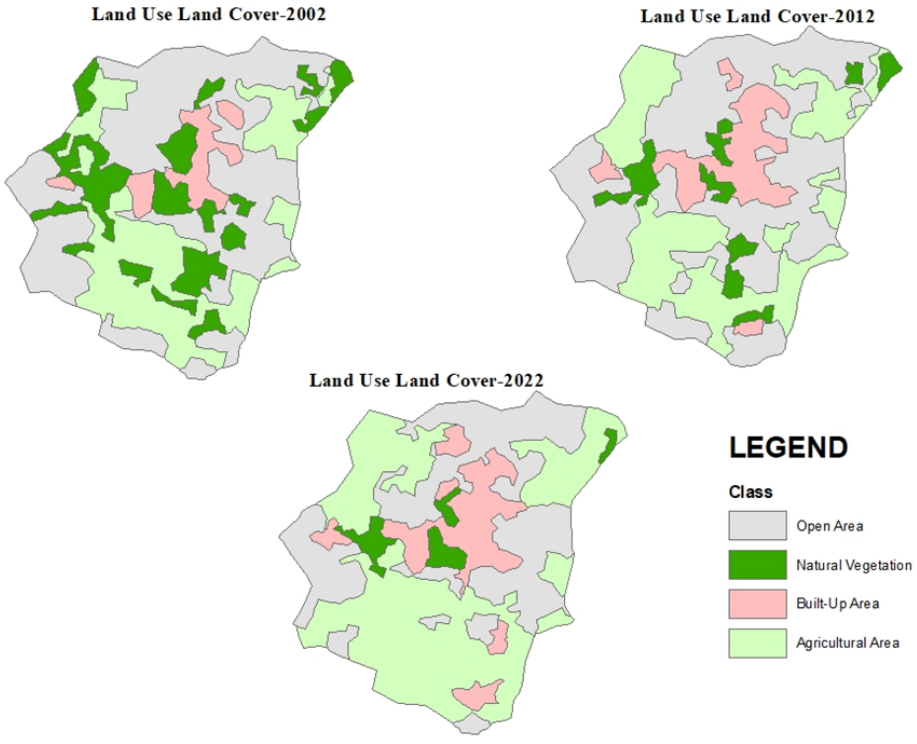

Figure 5. SVM classification of LULC map
S o u r c e : made by T. E. Sereke

2.2. Land Surface Temperature

The mean LST for the years 2002, 2012, and 2022 were 35.1, 30.2 and 31.8˚C, respectively, and the minimum and maximum ranges were 25.9–40, 2.2–39.6 and 23.7–38˚C, respectively (Figure 6). The mean LST decreased by 3.3˚C from 2002 to 2022 in the study area. Decreased mean LST was also reported by [9], but [2; 11; 12] reported increased mean LST due to built-up area increase. The overall mean LST in natural vegetation, agricultural, open, and built-up areas were 29.7, 32.8, 32.9 and 35.0˚C, respectively (Figure 7).

The built-up area recorded the highest mean LST, indicating the urban heat island effect [11; 12]. Natural vegetation had the lowest mean LST, which can be attributed to a cooling effect of vegetation.

The regression analysis showed that there was a negative correlation between NDVI and LST for the three years with R^2 values of 0.3041, 0.1038, and 0.4978 for 2002, 2012, and 2022, respectively.

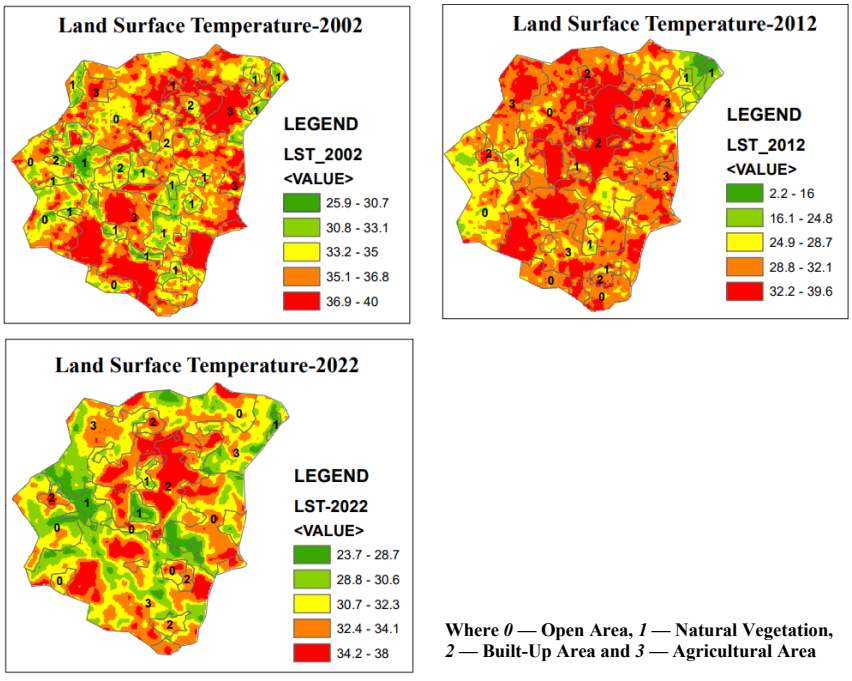

Figure 6. Spatial distribution of LST with LULC for 2002, 2012 and 2022
S o u r c e: made by T. E. Sereke

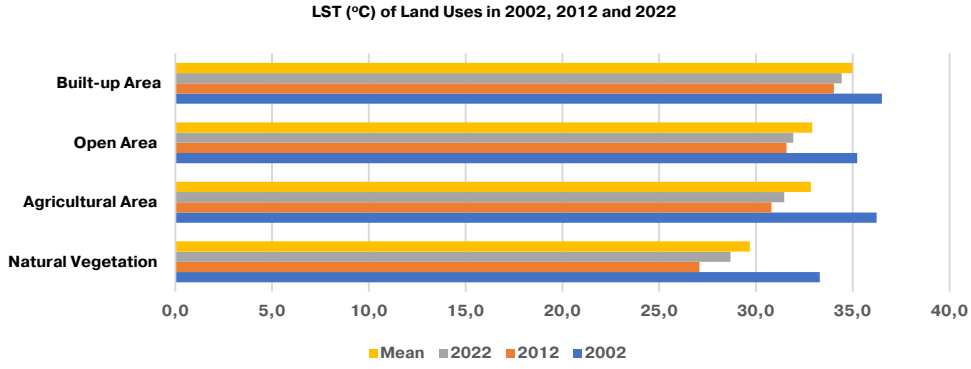

Figure 7. LST ˚C of Land Uses in 2002, 2012 and 2022
S o u r c e: made by T. Tesfay

Conclusion

The study employed remote sensing data and GIS techniques to examine, analyze and process the dynamics of LULC and evaluate their associated impacts on LST in Greater Mendefera, Eritrea, in 2002, 2012, and 2022. This study noted considerable LULC changes from 2002 to 2022 in the study area. Between 2002 and 2022, built-up and agricultural areas expanded by 113.5 and 64.4%, and on the contrary, natural vegetation and open areas shrank by 77.6 and 24.8%, respectively. The built-up area recorded the highest mean LST (35ºC), whereas the natural vegetation area had the lowest (29.7ºC). The mean LST decreased by 3.3˚C from 2002 to 2022 in the study area. This study could help policy makers in planning sustainable urban development to minimize urban heat island and global warming effects.

References

1. Amini S, Saber M, Rabiei-Dastjerdi H, Homayouni S. Urban Land Use and Land Cover Change Analysis Using Random Forest Classification of Landsat Time Series. *Remote Sens*. 2022;14(11):2654. https://doi.org/10.3390/rs14112654

2. Dissanayake DMSLB. Land use change and its impacts on land surface temperature in Galle city, Sri Lanka. *Climate*. 2020;8(5):65. https://doi.org/10.3390/CLI8050065

3. Dissanayake DMSLB, Morimoto T, Murayama Y, Ranagalage M. Impact of landscape structure on the variation of land surface temperature in Sub-Saharan Region: A case study of Addis Ababa using Landsat Data (1986–2016). *Sustainability*. 2019;11(8):2257. https://doi.org/10.3390/su11082257

4. Opelele OM, Yu Y, Fan W, et al. Analysis of the impact of land-use/land-cover change on land-surface temperature in the villages within the luki biosphere reserve. *Sustainability*. 2021;13(20). https://doi.org/10.3390/su132011242

5. Arsiso BK, Mengistu Tsidu G, Stoffberg GH, Tadesse T. Influence of Urbanization-Driven Land Use/Cover Change on Climate: The Case of Addis Ababa, Ethiopia. *Physics and Chemistry of the Earth*. 2018;10:212–223. https://doi.org/10.1016/j.pce.2018.02.009

6. Ibrahim GRF. Urban land use/land cover changes and their effect on land surface temperature: Case study using Dohuk City in the Kurdistan Region of Iraq. *Climate*. 2017;5(1). https://doi.org/10.3390/cli5010013

7. Hashim H, Latif ZA, Adnan NA. Land use land cover analysis with pixel-based classification approach. *Indonesian Journal of Electrical Engineering and Computer Science*. 2019;16(3):1327–1333. https://doi.org/10.11591/ijeecs.v16.i3.pp1327–1333

8. Basheer S, Wang X, Farooque AA, Nawaz RA, Liu K, Adekanmbi T, Liu S. Comparison of Land Use Land Cover Classifiers Using Different Satellite Imagery and Machine Learning Techniques. *Remote Sens (Basel)*. 2022;14(19):4978. https://doi.org/10.3390/rs14194978

9. Measho S, Chen B, Pellikka P, Trisurat Y, Guo L, Sun S, Zhang H. Land Use/Land Cover Changes and Associated Impacts on Water Yield Availability and Variations in the Mereb-Gash River Basin in the Horn of Africa. *J Geophys Res Biogeosci*. 2020;125(7):e2020JG005632. https://doi.org/10.1029/2020JG005632

10. Saharan MA, Vyas N, Borana SL, Yadav SK. Classification and Assessment of the Land Use — Land Cover Changes in Jodhpur City Using Remote Sensing Technologies. *The International Archives of the Photogrammetry, Remote Sensing and Spatial Information Sciences*. 2018;XLII-5:767–771. https://doi.org/10.5194/isprs-archives-xlii-5-767-2018

11. Rousta I, Sarif MO, Gupta RD, Olafsson H, Ranagalage M, Murayama Yu, Zhang H, Darlington Mushore T. Spatiotemporal analysis of land use/land cover and its effects on surface urban heat Island using Landsat data: A case study of Metropolitan City Tehran (1988–2018). *Sustainability*. 2018;10(12);4433. https://doi.org/10.3390/su10124433

12. Javaid K, Ghafoor GZ, Sharif F, Shahid MG, Shahzad L, Ghafoor N, Hayyat MU, Farhan M. Spatiotemporal analysis of land use/land cover change and its impact on land surface temperature of Sialkot City, Pakistan. *Nature/Scientific Reports*. 2023;13(1):22166. https://doi.org/10.1038/s41598-023-49608-x

13. Sam SC, Balasubramanian G. Spatiotemporal detection of land use/land cover changes and land surface temperature using Landsat and MODIS data across the coastal Kanyakumari district, India. *Geodesy and Geodynamics.* 2022;14(2023):172–181. https://doi.org/10.1016/j.geog.2022.09.002

14. Xue J, Su B. Significant Remote Sensing Vegetation Indices: A Review of Developments and Applications. *Journal of Sensors*. 2017(1):1–17. https://doi.org/10.1155/2017/1353691

15. Tewolde MG, Cabral P. Urban sprawl analysis and modeling in Asmara, Eritrea. *Remote Sens (Basel)*. 2011;3(10):2148–2165. https://doi.org/10.3390/rs3102148

16. Priyankara P, Ranagalage M, Dissanayake DMSLB, MorimotoT , Murayama Y. Spatial process of surface urban heat island in rapidly growing Seoul metropolitan area for sustainable urban planning using landsat

data (1996–2017). *Climate*. 2019;7(9):110. https://doi.org/10.3390/cli7090110

17. Sereke T, Bratkov V, Aristarkhova V. Allocation of land categories using the maximum likelihood algorithm based on landsat 8 images (using the example of the mendefera subzone, Eritrea). *Monitoring. Science & technologies.* 2023;2(56):63–69. https://doi.org/10.25714/MNT.2023.56.009

18. Anandababu D, Purushothaman BM, Suresh BS. Estimation of Land Surface Temperature Using LANDSAT 8 Data. *International Journal of Advance Research, Ideas and Innovations in Technology.* 2018;4(2):177–186. Available from: https://www.ijariit.com/manuscripts/v4i2/V4I2–1195.pdf (accessed:22.02.2024).

19. Sekertekin A, Bonafoni S. Land surface temperature retrieval from Landsat 5, 7, and 8 over rural areas: Assessment of different retrieval algorithms and emissivity models and toolbox implementation. *Remote Sens*. 2020; 12(2):294. https://doi.org/10.3390/rs12020294

About the authors

Temesghen E. Sereke, Ph.D student of the Department of Geography, Moscow State University of Geodesy and Cartography, Moscow, Russia; Lecturer II at the Department of Geography in College of Business and Social Sciences, Adi Keih, Eritrea; eLIBRARY SPIN-code: 2370-2028, ORCID: 0009-0001-1748-6479; e-mail: temesghensereke@gmail.com

Tumuzghi Tesfay**,** Ph.D student of the Department of Environmental Management, Institute of Environmental Engineering, RUDN University, Moscow, Russia; Lecturer II at Department of Land Resource in Hamelmalo Agricultural College, Keren, Eritrea; ORCID: 0000-0002-0771-5522; e-mail: tumuzghitesfay7@gmail.com

Vitaly V. Bratkov, Doctor of Geographical Sciences, Head of the Department of Geography, Moscow State University of Geodesy and Cartography, Moscow, Russia; eLIBRARY SPIN-code: 9691-2510; ORCID: 0000-0001-5072-1859; e-mail: vbratkov@mail.ru

Elsayed S. Mohamed**,** Professor of the Department of Environmental Management, specialized in soil sciences and remote sensing, Institute of Environmental Engineering, RUDN University, Moscow, Russia; Researcher of the Department Soil Science, National Authority for Remote Sensing and Space Sciences, Cairo, Egypt; ORCID: 0000-0001-5703-4621; e-mail: salama55@gmail.com

Dinh T. Quyen, PhD Student in the Faculty of Cartography, Department of Space Monitoring and Ecology, Moscow State University of Geodesy and Cartography, Moscow, Russia; ORCID: 0000-0002-6577-0087; e-mail: quyendinhtuyen97@gmail.com

Сведения об авторах

Сереке Темесген Эйяссу, аспирант географического факультета, Московский государственный университет геодезии и картографии, Москва, Россия; преподаватель, Колледж бизнеса и социальных наук, Ади Кейх, Эритрея; eLIBRARY SPIN-код: 2370-2028, ORCID: 0009-0001-1748-6479; e-mail: temesghensereke@gmail.com

Тесфай Тумузги**,** аспирант кафедры экологического менеджмента, Институт инженерной экологии, Российский университет дружбы народов, Москва, Россия; преподаватель, Сельскохозяйственный колледж Хамельмало, Керен, Эритрея; ORCID: 0000-0002-0771-5522; e-mail: tumuzghitesfay7@gmail.com

Братков Виталий Викторович, доктор географических наук, заведующий кафедрой географии, Московский государственный университет геодезии и картографии, Москва, Россия; eLIBRARY SPIN-код: 9691-2510, ORCID: 0000-0001-5072-1859; e-mail: vbratkov@mail.ru

Мохамед Эльсайд Саид, профессор кафедры экологического менеджмента, специалист по почвоведению и дистанционному зондированию, Институт инженерной экологии, Российский университет дружбы народов, Москва, Россия; научный сотрудник департамента почвоведения, Национальное управление по дистанционному зондированию и космическим наукам, Каир, Египет; ORCID: 0000-0001-5703-4621; e-mail: salama55@gmail.com

Куин Динь Туен, аспирант кафедры космического мониторинга и экологии, Московский государственный университет геодезии и картографии, Москва, Россия; ORCID: 0000-0002-6577-0087; e-mail: quyendinhtuyen97@gmail.com